Measurement of the increase in phase space density of a muon beam through ionization cooling

François Drielsma

University of Geneva

August 27, 2018

Table of contents

Path to slides: indico.cern.ch/event/739039 (PW: *muoncooling*)

State of the art
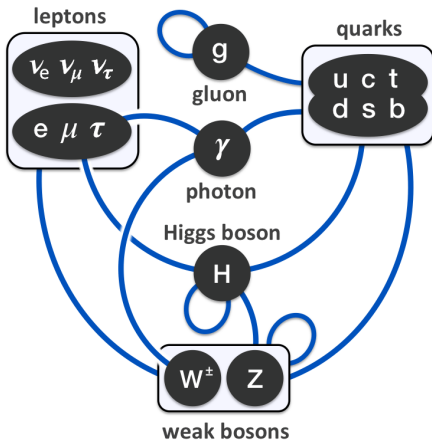
Standard Model

Most successful and predictive theory in the history of particle physics

Ties in **all three fundamental forces** relevant to the small scale: electromagnetic, weak and strong

Synergistic development of accelerator technologies and SM. Chronology:

○ Neutral current (Gargamelle @PS, 1973)

○ Charm, J/ψ (SLAC and BNL, 1974)

○ W and Z boson (S$p\bar{p}$S, 1983)

○ Z width (LEP, 1989-1994)

○ Top (Tevatron, 1995)

○ Higgs bosons (LHC, 2012)

Predictions of cross sections for particle production and decay processes with unprecedented accuracy
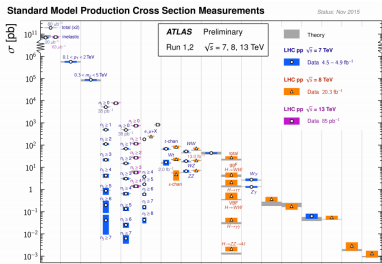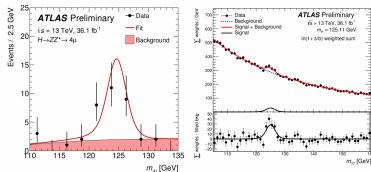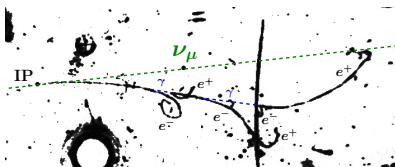
Beyond the Standard Model

The Standard Model is now complete... with some caveats:

- **No neutrino masses**
- No cold dark matter
- No matter/antimatter asymmetry

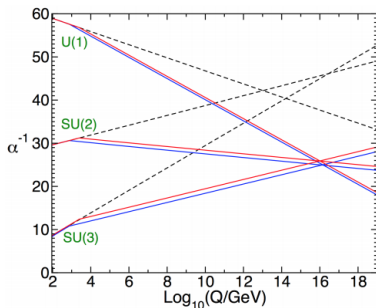$\rightarrow$ The theory must be extended to account for these experimental observations

The **neutrino minimal SM** (νMSM) is an attractive first extension:

- Adds heavy sterile RH neutrinos
- Provides DM candidate
- Provides baryogenesis explanation

Other possible extensions:

- SUSY (gauge coupling unification)
- Theory of Everything (add gravity)

Neutrino oscillations

Most compelling evidence of physics beyond SM in many channels:

- ν_e disapp. (C&R, SuperK and SNO)
- LBL $\bar{\nu}_e$ disapp. (KamLAND)
- ν_μ disapp., ν_e app. (T2K, NOνA)
- SBL $\bar{\nu}_e$ disapp. (DayaBay, RENO)

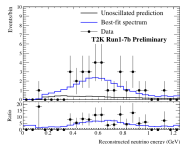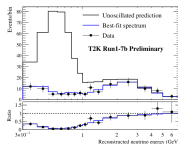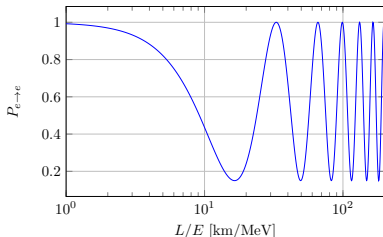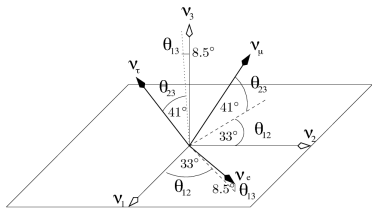This can only be explained if neutrinos have mass, mix through PMNS matrix:

$$\begin{pmatrix} 1 & 0 & 0 \\ 0 & c_{23} & s_{23} \\ 0 & -s_{23} & c_{23} \end{pmatrix} \begin{pmatrix} c_{13} & 0 & s_{13}e^{-i\delta} \\ 0 & 1 & 0 \\ -s_{13}e^{i\delta} & 0 & c_{13} \end{pmatrix} \begin{pmatrix} c_{12} & s_{12} & 0 \\ -s_{12} & c_{12} & 0 \\ 0 & 0 & 1 \end{pmatrix}$$

with $s_{ij} = \sin\theta_{ij}$ and $c_{ij} = \cos\theta_{ij}$.

Flavour states $\neq$ mass states,
$|\nu_\alpha\rangle = \sum_i U_{\alpha i}^* |\nu_i\rangle \iff$ Oscillations:
$$P_{\alpha \to \alpha} = 1 - \sin^2(2\theta)\sin^2\left(1.27\frac{\Delta m^2 L}{E}\frac{\text{GeV}}{\text{eV}^2 \cdot \text{km}}\right)$$

Neutrino properties

Mixing angles (2–3 %):

- $\theta_{12} = 33.62^{\circ +0.78^{\circ}}_{\ -0.76^{\circ}}$ (Solar+KamLAND)

- $\theta_{23} = 47.2^{\circ +1.9^{\circ}}_{\ -3.9^{\circ}}$ (T2K+NOνA+IceCube)

- $\theta_{13} = 8.54^{\circ +0.15^{\circ}}_{\ -0.15^{\circ}}$ (DayaBay+RENO)
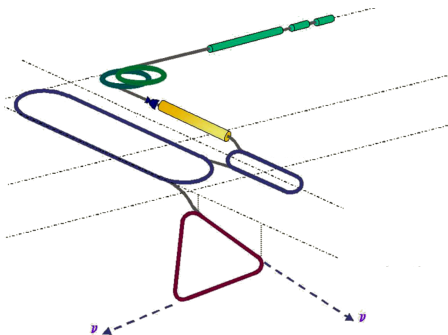
Mass splittings (1–3 %):

- $\Delta m^2_{12} = 7.40^{+0.21}_{-0.20} \times 10^{-5} \text{eV}^2$

- $\Delta m^2_{13} = 2.494^{+0.033}_{-0.031} \times 10^{-3} \text{eV}^2$ (NO)

What are we missing ?

- CP violating phase, δ (violation ?)

  - Violation preferred at 2–3 σ

- Mass ordering (normal/inverted ?)

  - Normal preferred at 3.5 σ

- Nature of neutrino mass
  (Majorana and/or Dirac ?)

- Heavy sterile neutrinos ?

NuFIT 3.2 (2018)
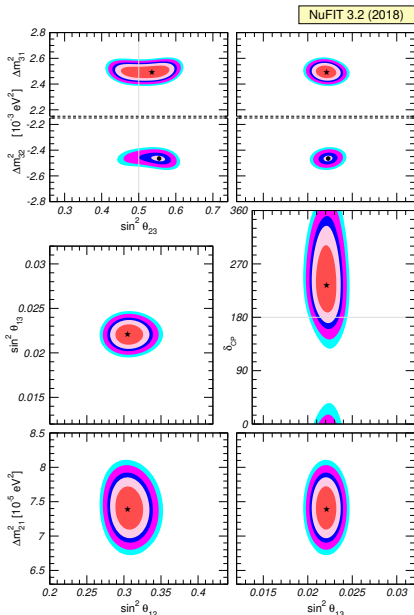
Muon-based facilities

Neutrino Factory

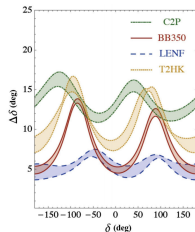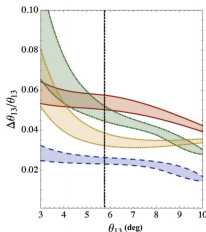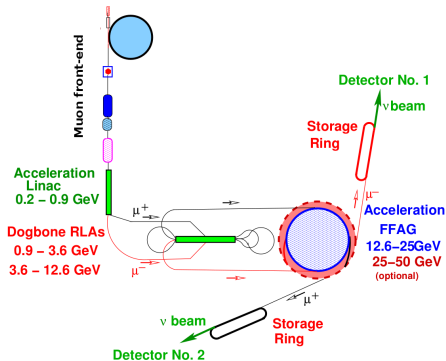**Simple idea**: use muon decays as an exquisitely clean source of neutrinos

- $\mu^+ \rightarrow e^+ + \nu_e + \bar{\nu}_\mu$
- $\mu^- \rightarrow e^- + \bar{\nu}_e + \nu_\mu$

Advantages over "super-beams":

- No wrong sign background
- Well known flux (Michel spectrum)
- Unprecedented $\nu_e/\bar{\nu}_e$ flux

Precision era of neutrino physics:

- 0.5% on Δm_{13}^2
- Guaranteed CPV ($\pm 5°$ on δ, = CKM)
- Guaranteed mass hierarchy at 5σ
- Test PMNS unitarity ($\nu_e \rightarrow \nu_\tau$)
- **Cross-section better than 1%**

Muon Collider, energy frontier

**Energy frontier** ($\rightarrow 100\,\text{TeV}$):

- Higher energy and unprecedented precision tests of the SM

- Extend search for supersymmetry

- Running of coupling constants

- Discovery of dark matter

Circular e^+e^- colliders limited by synchrotron radiation. Radiated power:

$$P = \frac{1}{m^4} \frac{e^4 E^2 B^2}{6\pi\epsilon_0 c^5}.$$

$\mu^\pm$ $200\times$ heavier than $e^\pm$, loose energy $\sim 10^9$ **times** less:

- Higher energy reach (frontier)

- Higher luminosity/MW for $> 1\,\text{TeV}$

- Smaller footprint, easier staging
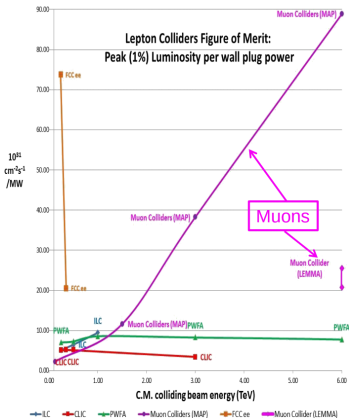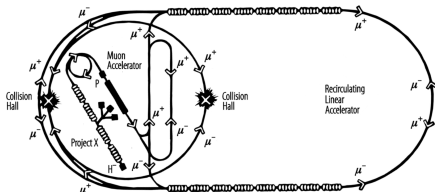
Muon Collider as Higgs factory

SM Higgs candidate at the LHC:

- Mass of $125.09 \pm 0.24 \, \text{GeV}/c^2$
- Width $< 0.013 \, \text{GeV}/c^2$ at 2σ C.L.
- Z, W, b, τ, γ couplings to 2-10 %
- Even integer spin

$\rightarrow$ Will need a **lepton machine** to significantly improve resolution on couplings and width as it may contain hints of physics beyond the SM

Muon Collider:
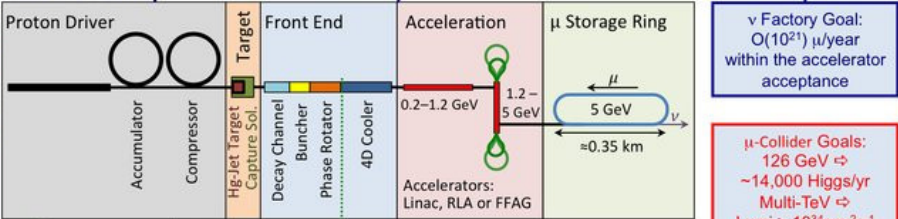
- Larger muon coupling allows for Higgs production through s-channel
- $\sigma \simeq 40 \, \text{pb}$, same as LHC at $14 \, \text{TeV}$
- $\sim \text{MeV}$ resolution on Higgs width
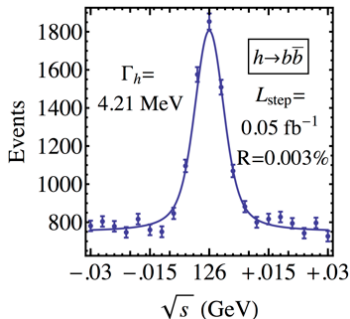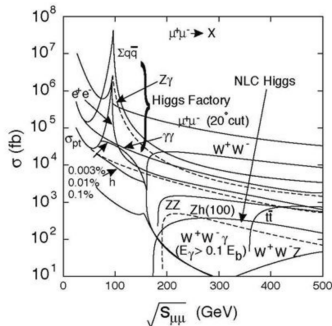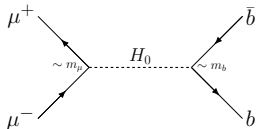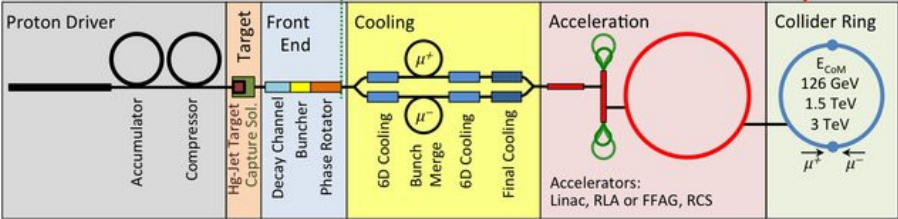
Neutrino Factory and Muon Collider front-ends

Both facilities share the same front-end, both require the **hot muon beam** produced from pion decays to be **cooled significantly**.
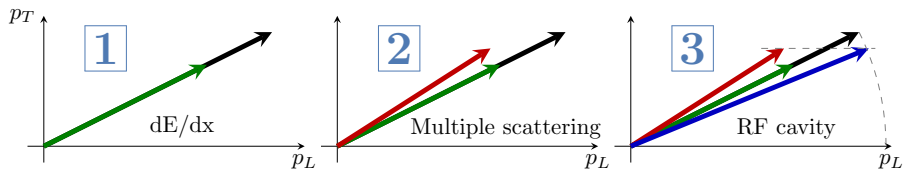
Principle of ionization cooling

Only viable method to cool a muon beam within muon lifetime ($\sim 2.2\,\mu$s)

1. the energy loss, dE_μ/dz, reduces p_L and p_T;
2. the multiple scattering increases the angular spread;
3. RF cavities restore p_L only, effectively reducing the angular spread.

Rate of transverse normalised emittance change approximated by:

$$\frac{d\epsilon_\perp}{dz} \simeq \underbrace{-\frac{1}{\beta^2}\frac{\boldsymbol{\epsilon_\perp}}{E_\mu}\left|\frac{dE_\mu}{dz}\right|}_{\textbf{Cooling}} + \underbrace{\frac{(13.6\,\text{MeV})^2}{2\beta^3 E_\mu m_\mu c^2}\frac{\boldsymbol{\beta_\perp}}{\boldsymbol{X_0}}}_{\textbf{Heating}}$$

$\rightarrow$ Minimize $\boldsymbol{\beta_\perp/X_0}$ by placing a **low Z absorber at a tight focus**.

Muon Ionization Cooling Experiment (MICE)

MICE designed as a **proof-of-principle** of ionization cooling. Goals:

- build and operate a realistic section of a cooling channel;
- measure a significant increase in phase space density of a muon beam.

Comprehensive set of instruments:

- Thorough particle identification system to select muons
  - Time-of-flight detectors, Cherenkov threshold counters and calorimetry
- Scintillating fibre trackers to reconstruct phase space of muons

Cooling channel section comprises a single low Z absorber module (LiH or LH_2) placed at the focal point of a pair of superconducting magnets.
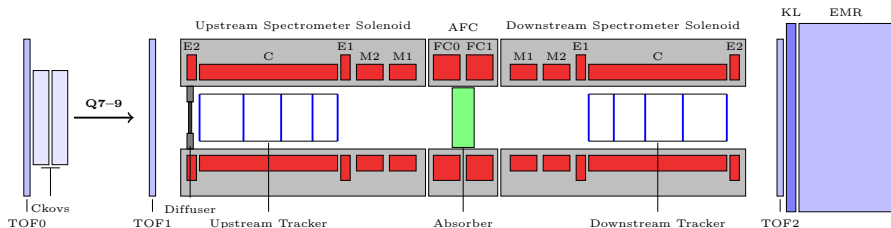
MICE in pictures
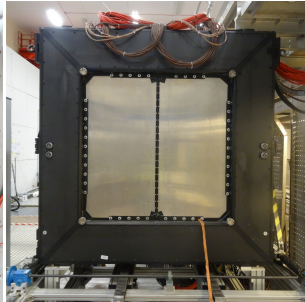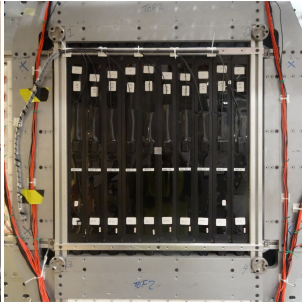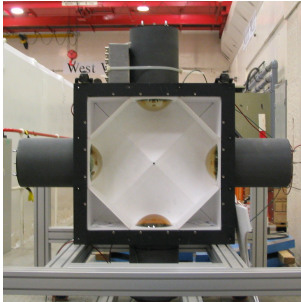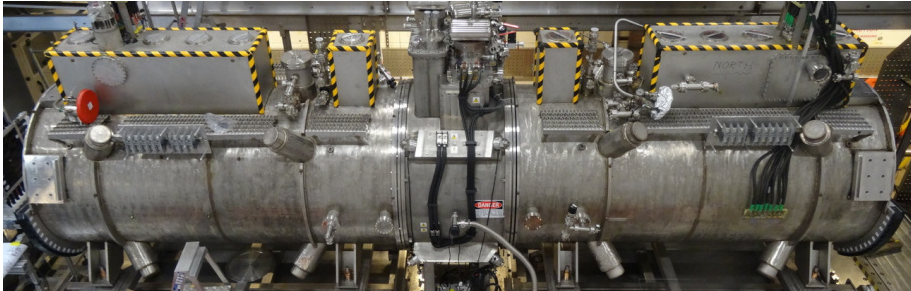
Muon beam

MICE operates parasitically on the 800 MeV ISIS p^+ synchrotron at RAL
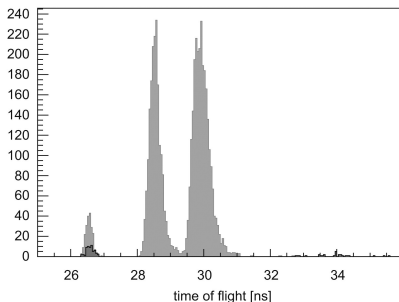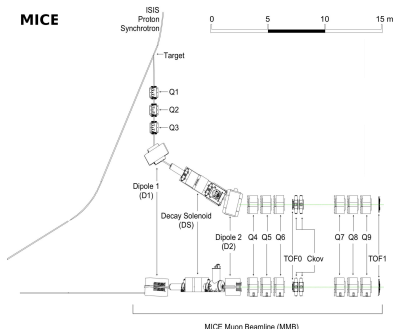
- Ti target dipped in p^+ beam halo
- π^+ momentum selected at D1
- $\pi^+ \to \mu^+ + \nu_\mu$ decays between D1 and D2
- μ^+ momentum selected at D2

Beam line typically set to select same momentum at D1 and D2 (*pionic*)

At momenta of 140–240 MeV/c, time-of-flight very strong identification variable:

$$\frac{t_\mu}{t_\pi} = \frac{E_\mu}{E_\pi} = \frac{\sqrt{1 + m_\mu^2 c^2/p^2}}{\sqrt{1 + m_\pi^2 c^2/p^2}}$$

EMR rejects muon decays in flight (JINST 10 (2015) P12012)

Single-particle experiment

MICE is a single-particle experiment, i.e.

- There is no "beam" as such going down the beam line, particles pass through the experiment one by one ($f \sim 200\,\mathrm{kHz}$ for $1\,\mathrm{ms}$ every $1\,\mathrm{s}$)
- At each DAQ cycle, a **single particle track** is recorded
- Particle tracks are bunched at the analysis level to create an **ensemble** of which to reconstruct the phase space distribution

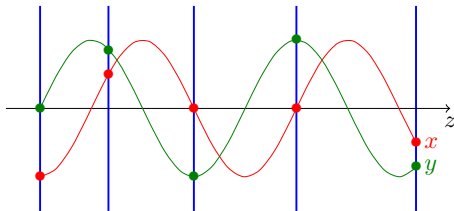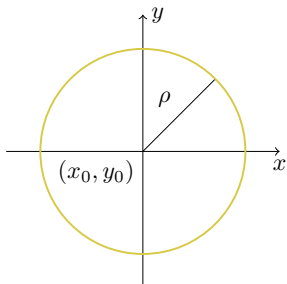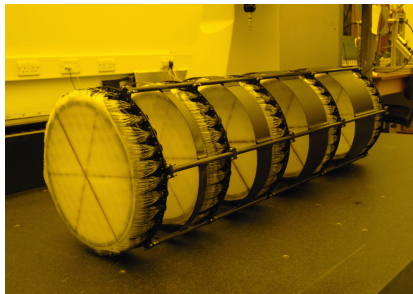$\rightarrow$ First **direct measurement** of the full phase space of muons with scintillating fibre-trackers
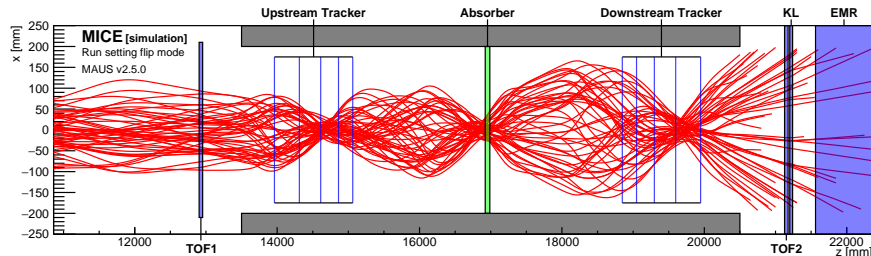
Phase space reconstruction

Coordinates of muon, (x, y, p_x, p_y, p_z), reconstructed by fitting helix to muon path inside a uniform solenoid field:

- $p_T = qB_z\rho$
- $p_z = p_T / \sqrt{(ds/dz)^2 - 1}$

Position resolution in each station:

- $\sigma_{x,y} = 467 \pm 2 \,\mu\mathrm{m}$
- $\sigma_{p_T} \simeq 1.3 \,\mathrm{MeV}/c$, $\sigma_{p_z} \simeq 4 \,\mathrm{MeV}/c$
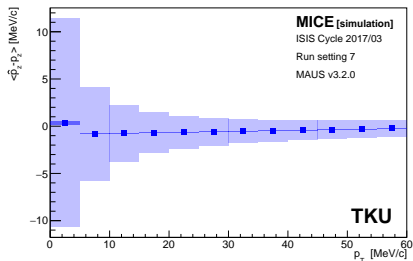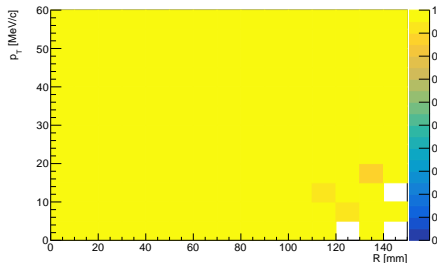
Tracker p_z resolution

The trackers are highly efficient. If a muon goes through their fiducial volume, they almost certainty record a track (*bottom left*).

At low p_T, however, the p_z resolution is poor (*bottom right*)

$\rightarrow$ If one applies a momentum cut to preserve monochromaticity, one will inevitably **loose more low p_T tracks**;

$\rightarrow$ It creates a **hole** at the centre of the phase space which hinders any hope of recovering an unbiased phase space density.

Time-of-flight approach

The low p_z resolution is an **inherent limitation** of the tracker technology. If the radius is too small, the uncertainty diverges.
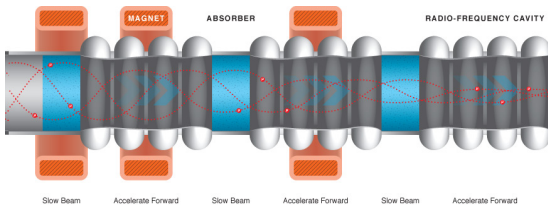
ToF of $\sim 140\,\mathrm{MeV}/c$ particles offers exquisite estimate of p ($\sim 0.5\,\%$):
  $\rightarrow$ Use it to recover the phase space of low p_T tracks;
  $\rightarrow$ Only real uncertainty is energy straggling, worse for large $\epsilon_\perp$ beams;
  $\rightarrow$ Use the weighted momentum estimate, scale accordingly.

For the downstream section, propagate the total momentum downstream. Once again, use the weighted average.
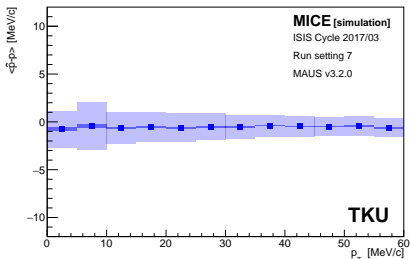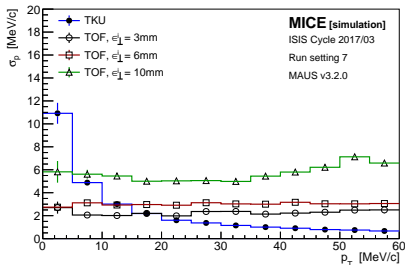
Cooling measurement

Cooling channel settings under consideration

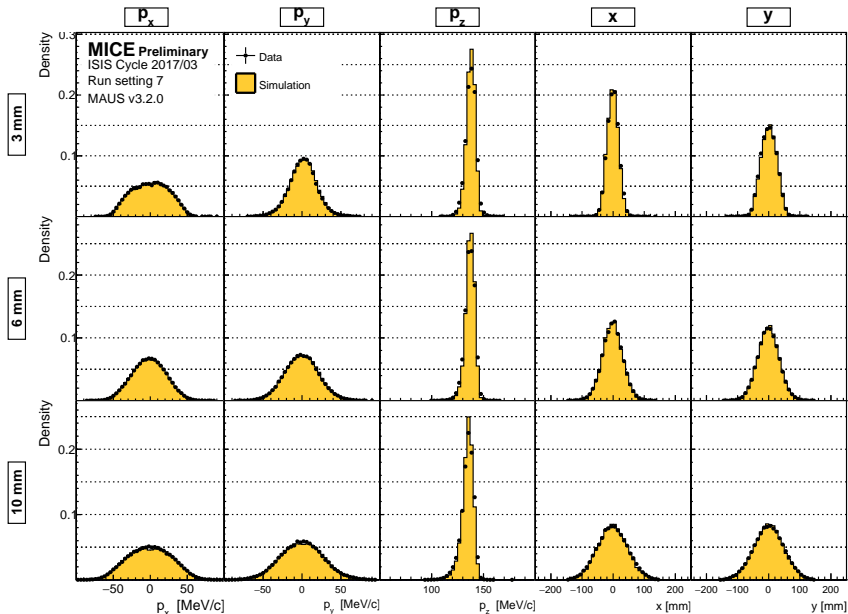MICE recorded data in a broad set of configurations:

- 4 input $\epsilon_\perp$, 4 momenta, 8 magnet settings (> 100 configurations)

Analysis focused on the **140 MeV/c** data sets taken with the **LiH** absorber

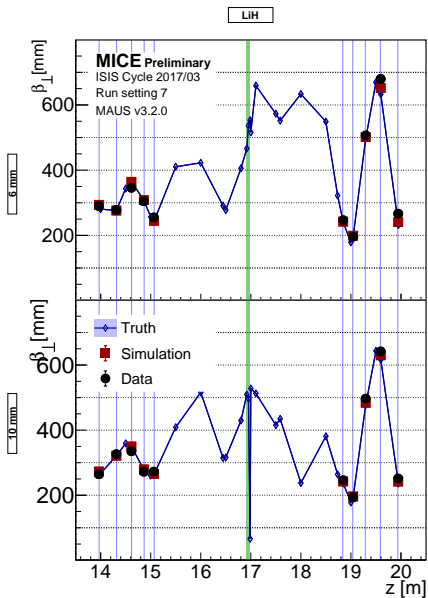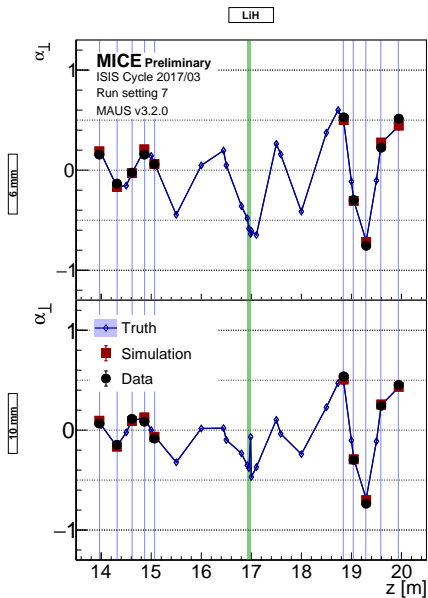|	2016/04-1.2	2016/05-1	**2017/02-7**
Mode	Solenoid	Flip	**Flip**
Momentum [MeV/c]	140	140	**140**
Emittances [mm]	3, 6, 10	3, 6, 10	**3, 6, 10**
$\beta_\perp^*$	~ 800 mm	~ 550 mm	**$\sim$520 mm**
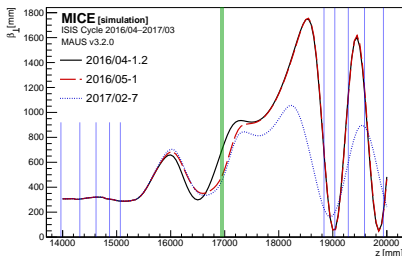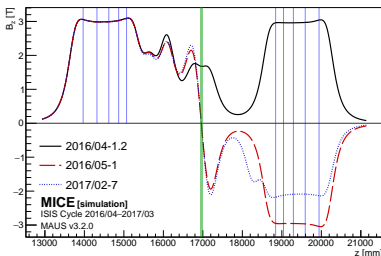
Upstream profiles

Downstream profiles
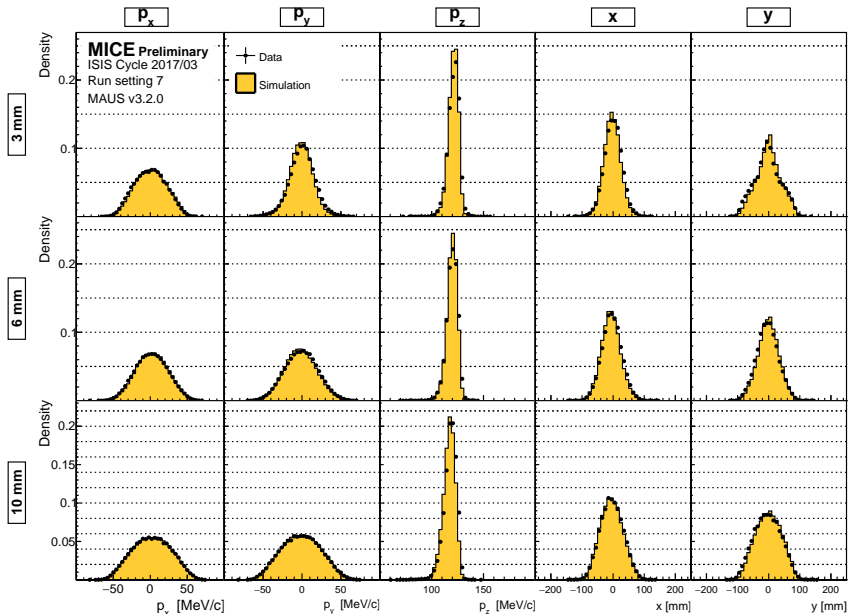
Optical functions

Transverse normalised RMS emittance

Transverse normalised RMS emittance defined as

$$\epsilon_\perp = \frac{1}{m}|\mathbf{\Sigma}_\perp|^{\frac{1}{4}},$$

with $|\mathbf{\Sigma}_\perp|$ the determinant of the covariance matrix.

The RMS emittance is directly related to the **volume of the RMS ellipsoid** through $\epsilon_\perp = \sqrt{2V_{\mathsf{RMS}}}/(m\pi)$ and as such is the most common probe of average phase-space density.

Limitation: Poor estimate if low transmission or non-linear transport
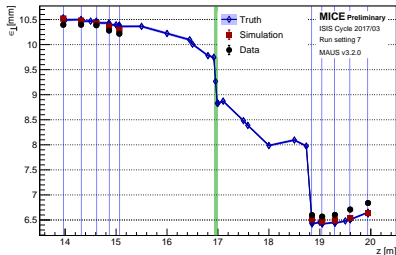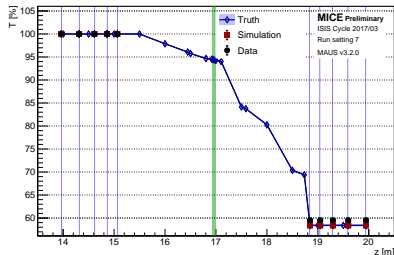
Transverse single-particle amplitude

Single particle amplitude is defined as

$$A_\perp = \epsilon_\perp \mathbf{u}^T \mathbf{\Sigma}_\perp^{-1} \mathbf{u} \equiv \epsilon_\perp R^2,$$

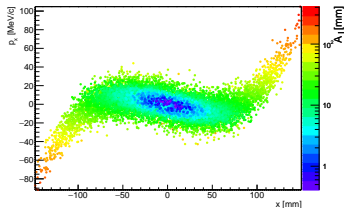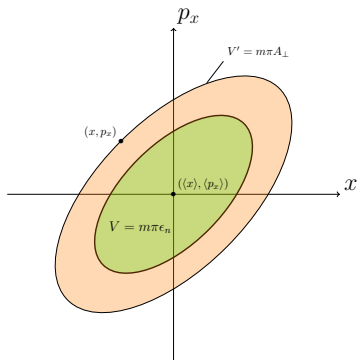with $\mathbf{u} = \mathbf{v} - \boldsymbol{\mu}$, the centered phase-space vector of the particle.

It is related to the **volume** of an ellipse similar to the RMS ellipse, going through $\mathbf{v}$.

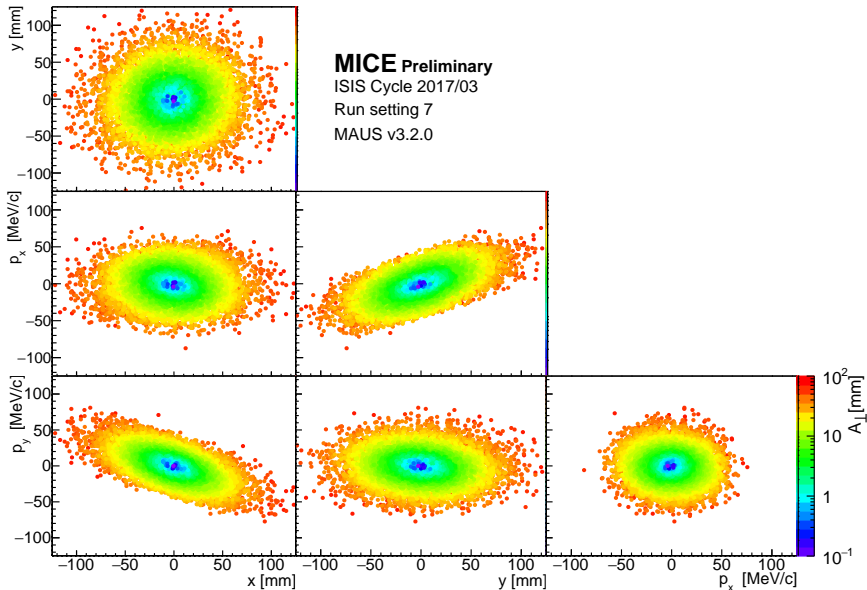High amplitudes **iteratively removed** from ensemble to prevent bias

Particle amplitude closely related to density in a Gaussian beam:

$$\rho(\boldsymbol{v}_i) = \boxed{\rho_{\mathsf{max}} \exp\left[-A_\perp/(2\epsilon_\perp)\right]}.$$
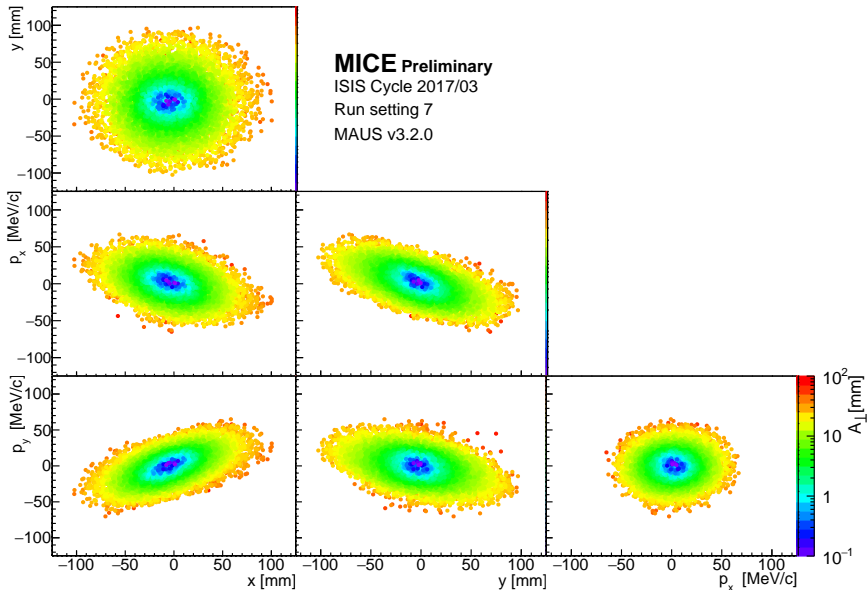
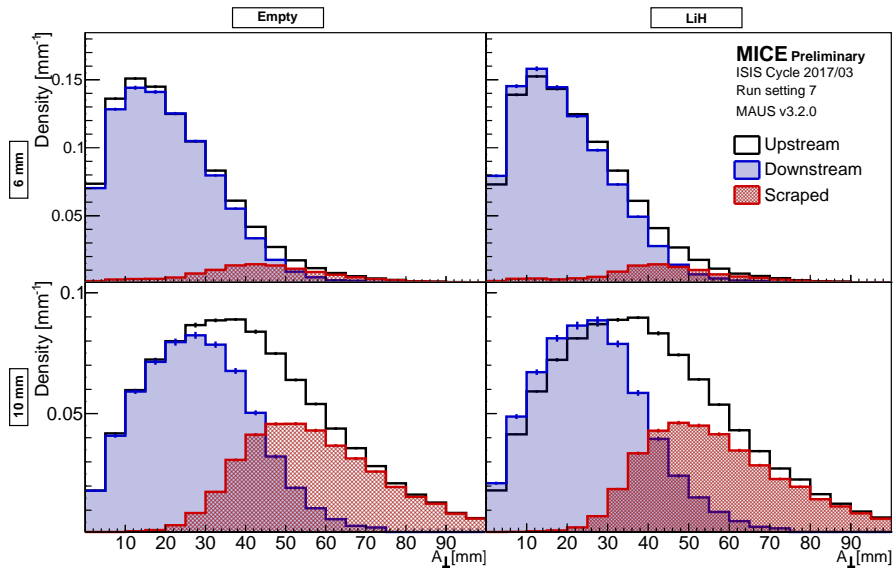$\rightarrow$ Allows for selection of **high density core**

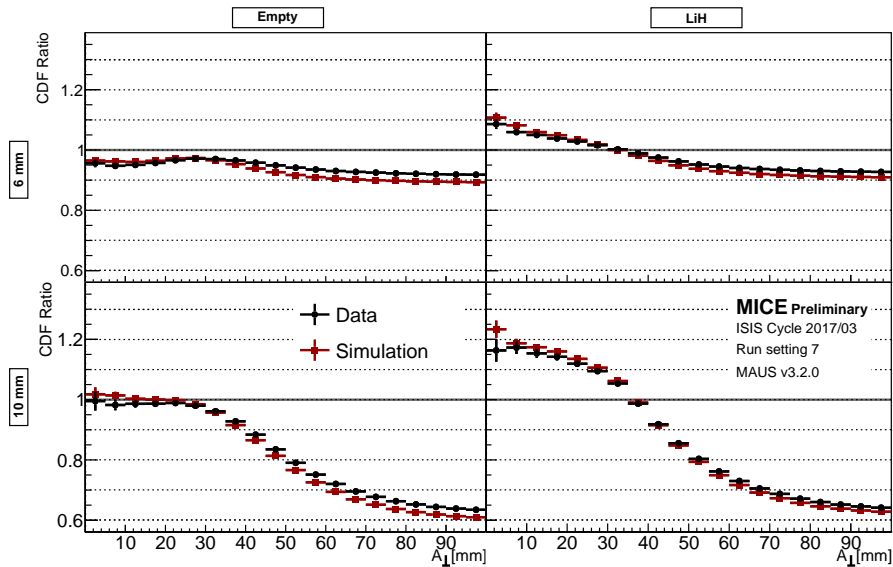# Poincaré sections upstream (6 mm, LiH)

Poincaré sections downstream (6 mm, LiH)

Amplitude distributions in data

CDF ratios

Summary statistics

Several summary statistics studied and viable, as summarized here:

	A_α	e_α	ϵ_α
Name	α-amplitude	α-subemittance	α-emittance
Meaning	Quantile of $A_\perp$ dist.	$\epsilon_\perp$ of core	Volume of core
Value	$\epsilon_\perp \chi_4^2(\alpha)$	$\epsilon_\perp P(3, \chi_4^2(\alpha)/2)/\alpha$	$\frac{1}{2}m^2\pi^2\epsilon_\perp^2\chi_4^2(\alpha)$
$\alpha = 9\%$	$\epsilon_\perp$	$\sim 0.16\epsilon_\perp$	V_{RMS}
σ_x/x	$g(\alpha)\sqrt{\alpha(1-\alpha)/n}$	$1/\sqrt{2\alpha n}$	$2g(\alpha)\sqrt{\alpha(1-\alpha)/n}$
$\alpha = 9\%$	$\sim 1.9/\sqrt{n}$	$\sim 2.4/\sqrt{n}$	$\sim 3.8/\sqrt{n}$
$\Delta x/x$	δ	δ	$(\delta+1)^2 - 1 \simeq 2\delta$

- $P(n, x)$ the regularized Gamma function;
- $g(\alpha)$ a complicated function of α (see dissertation);
- δ is the relative normalised emittance change.

A fraction of $\alpha = 9\%$ **is chosen** as it represents the RMS ellipse in 4D.

Fractional emittance evolution
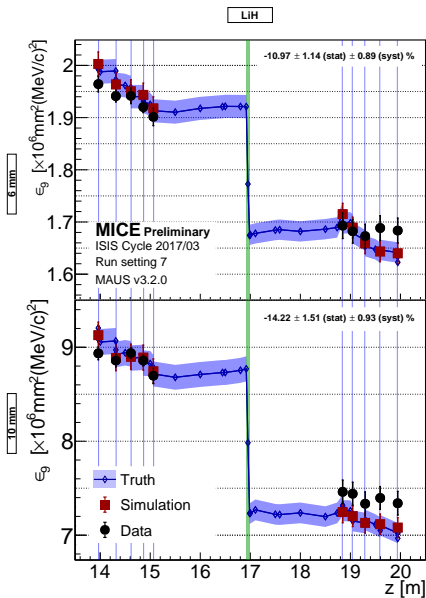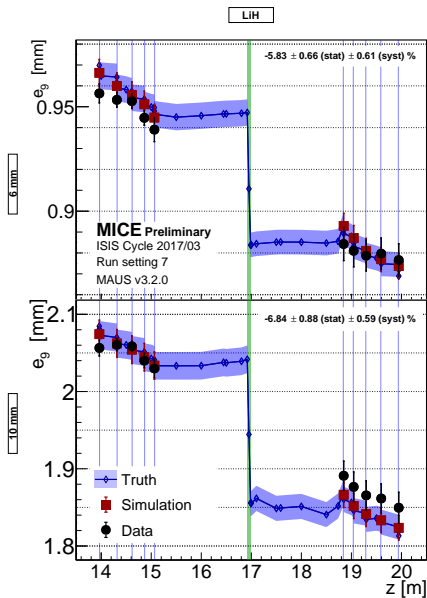
Nonparametric density estimation

Amplitude methods work well for beams with a **Gaussian core**.
Nonparametric DE removes prior assumption on underlying distribution.

Three classes of estimators considered for this measurement

	Histograms	k-Nearest Neighbour	PBATDE
$\rho(\boldsymbol{x})$	$n_i(\boldsymbol{x})/(n\Delta_i)$	$k/(n\kappa_d R_k^d)$	$\frac{1}{M}\sum_{i=1}^{M} \upsilon_i^{-1}$
MISE	$\mathcal{O}(\Delta^{2/d} + 1/(n\Delta))$	$\mathcal{O}((k/n)^{4/d} + 1/k)$	$\mathcal{O}(J^{-4/d} + J/n)$
$d=4$	$\mathcal{O}(\Delta^{1/2} + 1/(n\Delta))$	$\mathcal{O}(k/n + 1/k)$	$\mathcal{O}(1/J + J/n)$
Convergence	$n^{-2/(2+d)}$	$n^{-4/(4+d)}$	$n^{-4/(4+d)}$
$d=4$	$n^{-1/3}$	$\boldsymbol{n^{-1/2}}$	$\boldsymbol{n^{-1/2}}$
Speed	**Fast**	**Fast**	Slow

k-**Nearest Neighbour** (kNN) estimator has highest rate of convergence
(on par with the PBATDE) and is the least computationally intensive.

Systematic studies on a broad array of distribution classes showed
robustness of the kNN algorithm (see dissertation).

k-Nearest Neighbor

To find the density at a point $\boldsymbol{x}$ in phase space, find the k closest data points, with the distance defined as

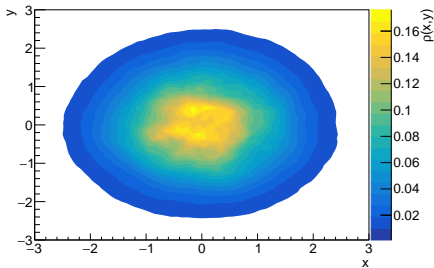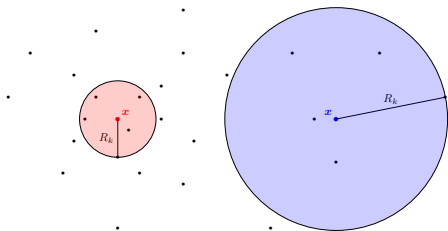$$D_i^2 = (\boldsymbol{x} - \boldsymbol{x}_i)^T(\boldsymbol{x} - \boldsymbol{x}_i), \qquad (1)$$

the Euclidean distance.

If R_k is the distance to the kth point, the 4D density then reads

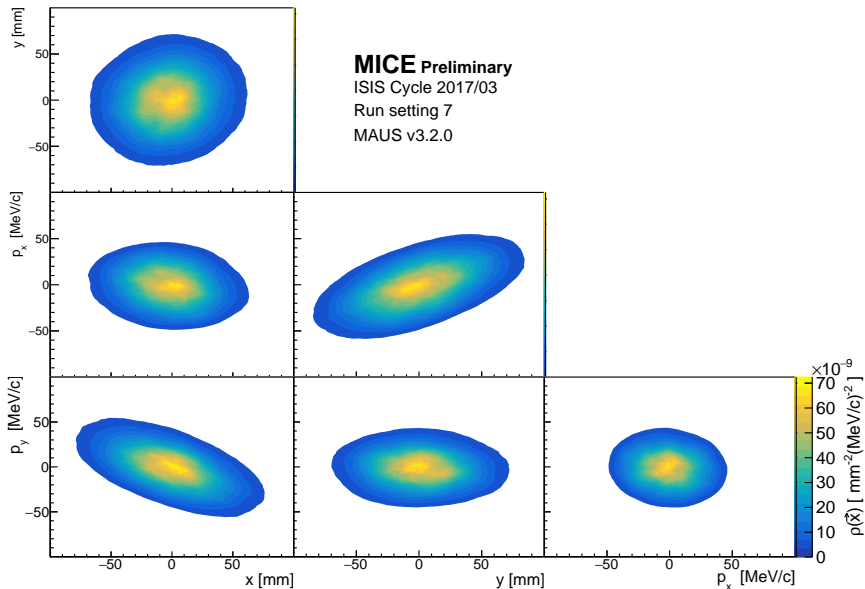$$\rho(\boldsymbol{x}) = \frac{k}{n}\frac{1}{\kappa_4 R_k^4}, \qquad (2)$$

with $\kappa_4 = \pi^2/2$, the volume of the Euclidean unit 4-ball.
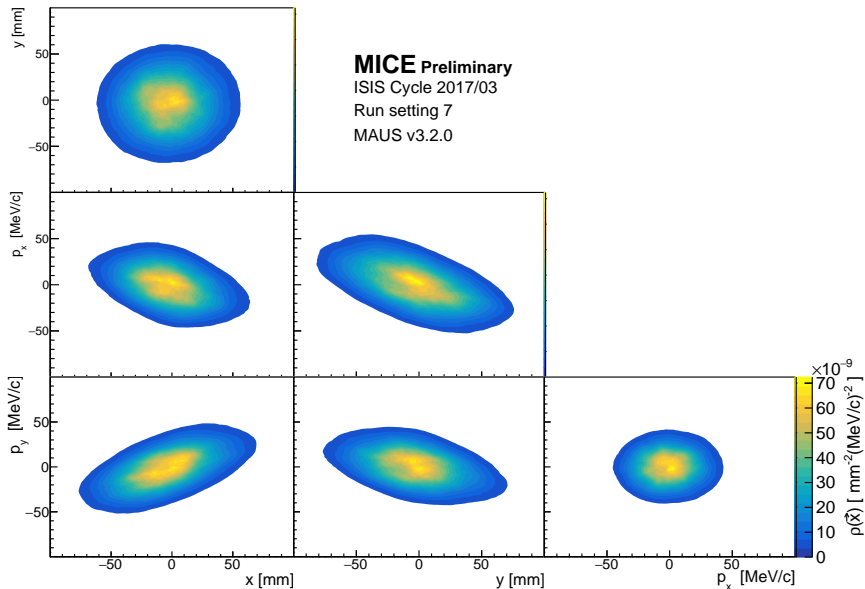
The optimal k in 4D follows $k \sim \sqrt{n}$.

kNN density of 10^3 Gaussian points

kNN Poincaré sections upstream (6 mm, LiH)

# kNN Poincaré sections downstream (6 mm, LiH)

Contour levels

**Goal**: Need a 1D density profile of the a 4D phase space to compare the output to the input.

Challenge: The probability density function is unknown; the concept of amplitude is meaningless. Must find a different quantity.

Solution: Contour levels. For a core fraction α, find the level of the corresponding contour. If the level has raised at a given α, the density of particles has increased. With F^{-1} the inverse CDF,

$$\rho_\alpha = \rho(F^{-1}(\alpha)). \qquad (3)$$
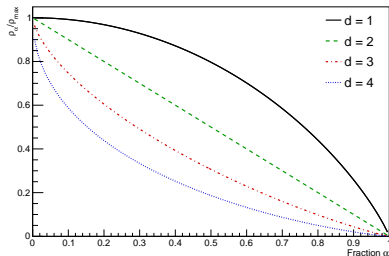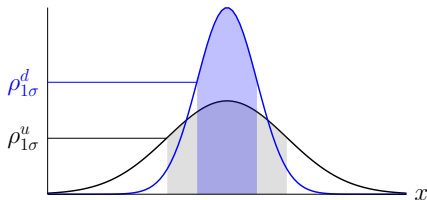
Density profiles in data
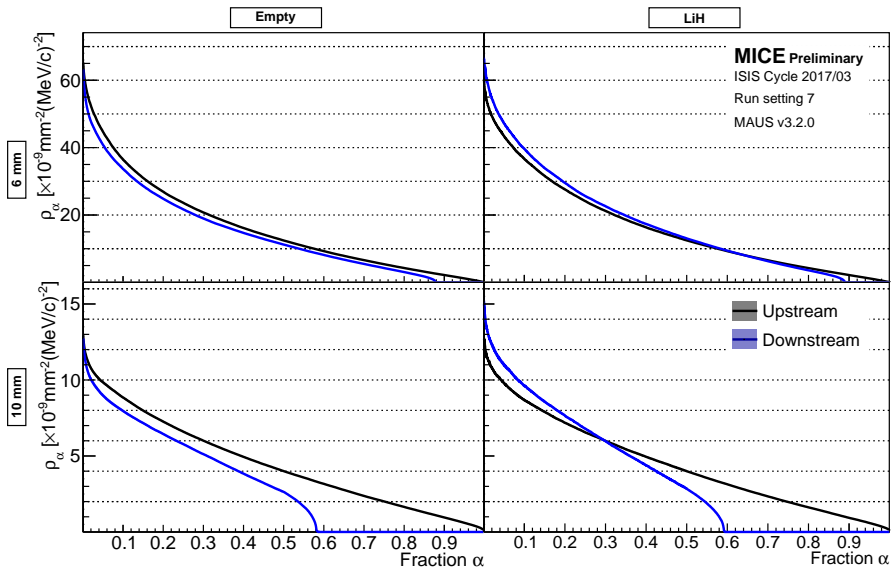
Density level evolution

As a summary statistic, represent evolution of arbitrary contour level → **9 % as it corresponds to the RMS ellipse contour**, ρ_9.
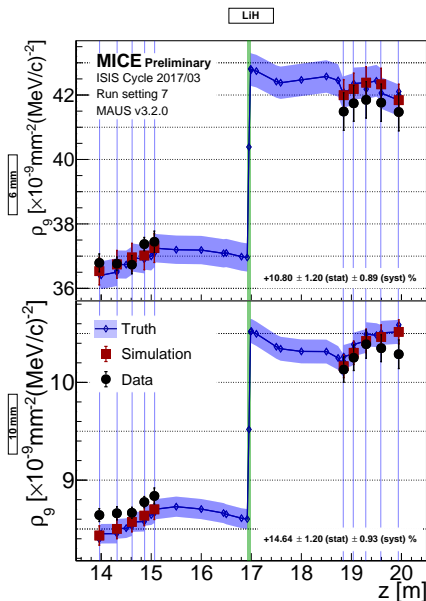
If beam core Gaussian, ratio reads

$$\frac{\rho_\alpha^d}{\rho_\alpha^u} = \frac{|\mathbf{\Sigma}_\perp^u|^{\frac{1}{2}}}{|\mathbf{\Sigma}_\perp^d|^{\frac{1}{2}}} = \left(\frac{\epsilon_\perp^u}{\epsilon_\perp^d}\right)^2$$

and the relative change

$$\frac{\rho_\alpha^d - \rho_\alpha^u}{\rho_\alpha^u} = \frac{1}{(\delta+1)^2} - 1 \simeq -2\delta$$

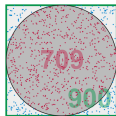with δ the relative RMS emittance change. If emittance decreases by δ, density increases twice as much.

Contour volume evolution

Alternative is to compute the **volume of phase space** that contains the particles above ρ_9, V_9, the generalised fractional emittance.

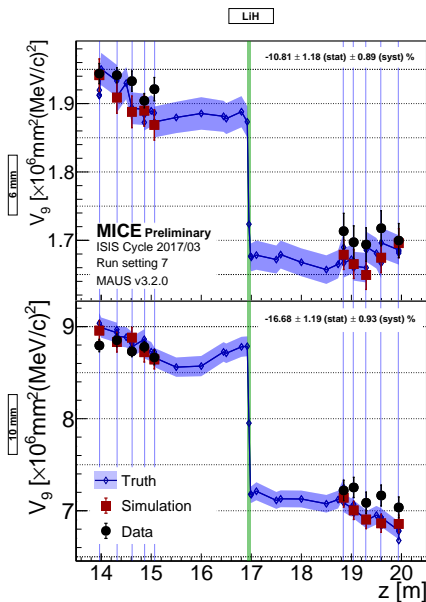Pick n points inside 4D box, particle for which $\rho > \rho_\alpha$ inside contour. Contour volume:

$$V_\alpha = n(\rho > \rho_\alpha)V_{box}/n$$

For Gaussian, relative change:

$$\frac{V_\alpha^d - V_\alpha^u}{V_\alpha^u} = (\delta + 1)^2 - 1 \simeq \mathbf{2}\delta$$

$\rightarrow$ Same as fractional emittance.

Conclusions

1. **First measurement** of the increase of phase space density of a muon beam through ionization cooling.

2. **Consistent measurements** achieved using the concept of particle amplitudes and nonparametric density

3. **Excellent agreement** between the observed phase space volume reduction, the simulations and the models
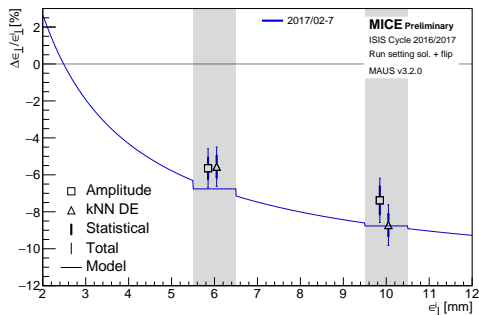

Figure: *Relative emittance change of muon beams through a 65 mm-thick LiH absorber disk, as reconstructed from the volume of the transverse RMS ellipsoid.*

With this measurement, we have shown that the number of muons inside the acceptance of an accelerator could be increased by ionisation cooling, and that the simulations at hand agree well with the data

This is a small but important step towards the realization of high brilliance muon storage rings (muon decay neutrino beams, and muon colliders)

Thank you to all those who, for many years, contributed to this result !

Backup slides

Neutrino Factory 4D cooling section

The **80 m cooling section** in the design study (arXiv:1112.2853) contains **fifty 1.5 m cooling cells** of

$4\times$ 1.5 cm-thick LiH absorbers;

$4\times$ 25 cm RF cavities;

$2\times$ 2.8 T solenoids in flip mode.

The LiH absorbers provide the energy loss and the RF cavities restore p_L.

The solenoids provide a ~ 0.8 m $\beta_\perp$ function focus at the absorbers.

Overall, the front-end increases the capture rate of muons in the accelerator acceptance **by a factor 10**.

Transverse emittance, muons, G4beamline and ICOOL
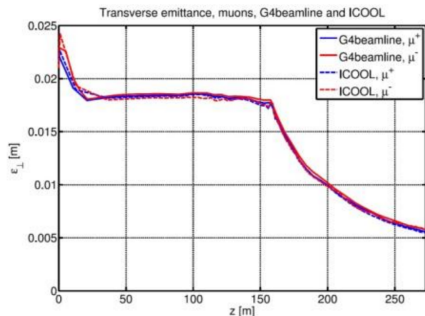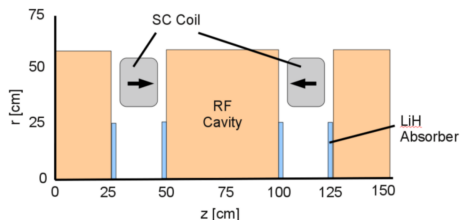
Muon Collider 6D cooling section

The 6D cooling section in the numerical study (PhysRevSTAB.18.031003) has an initial four stages over 380 m, followed by a bunch merger and eight additional stages over 500 m.

Each stage incrementally decreases its equilibrium emittance. The first stage consists of 66 cells of

- $2\times$ LH$_2$ wedge absorbers;
- $6\times$ 25.5 cm RF cavities;
- $2\times$ 2.4 T solenoids in flip mode.

Finally, reverse emittance exchange may be used to reach the luminosity required for a multi-TeV collider.
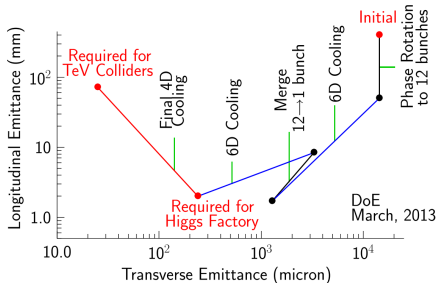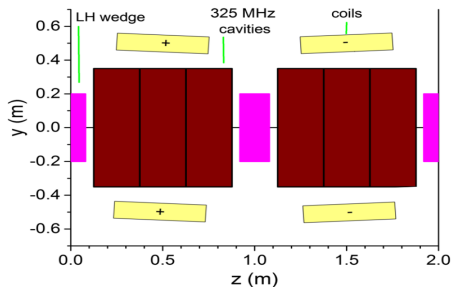
Simulations

Using the MAUS 3.2.0 simulations (latest, thanks DR, DM and PF)

- ○ $\sim 100k$ particles per setting, D2 tuned up to match observed;
- ○ High ρ glue in trackers, matched within the tracker reconstruction;
- ○ Fields scaled up by 1.8% in SSU and 1.55% in SSD to match the hall probe measurements;
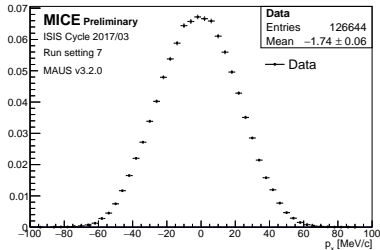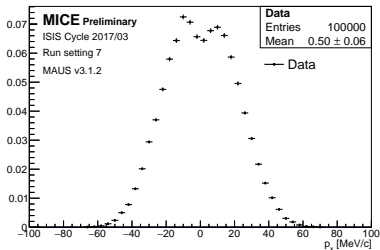- ○ Hall probe readings stable at the 10^{-4} level between runs.
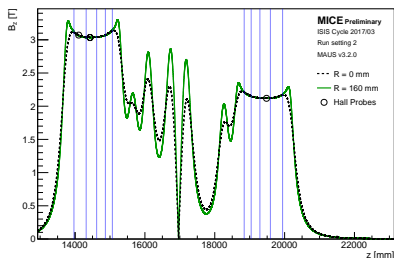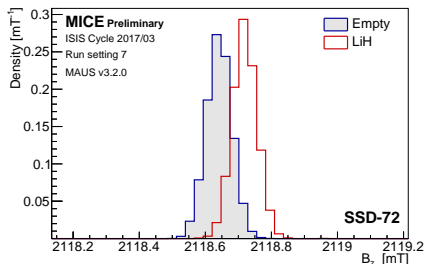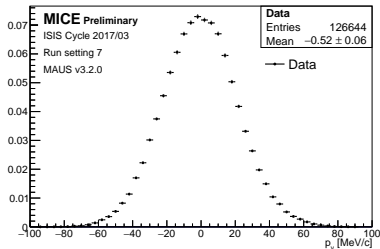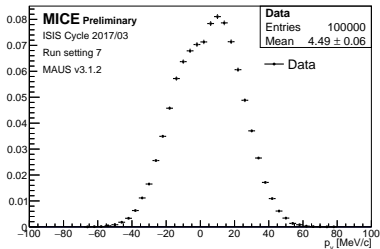
# Comparison of the 6 mm beam, TKU S1

Before fix

After fix

p_x

p_y

Sample selection

Series of selection criteria applied to the data and the simulation:

- 1 SP in TOF0
- 1 SP in TOF1
- ToF01 compatible with μ
- 1 tracker track (**TKU+TKD**)
- $\chi^2/\text{ndf} < 10$ (**TKU+TKD**)
- Fiducial radius < 150 mm (**TKU+TKD**)
- TKU total momentum $\in [135, 145]$ MeV/c
- Energy loss between TOF1 and TKU compatible with μ and true diffuser thickness
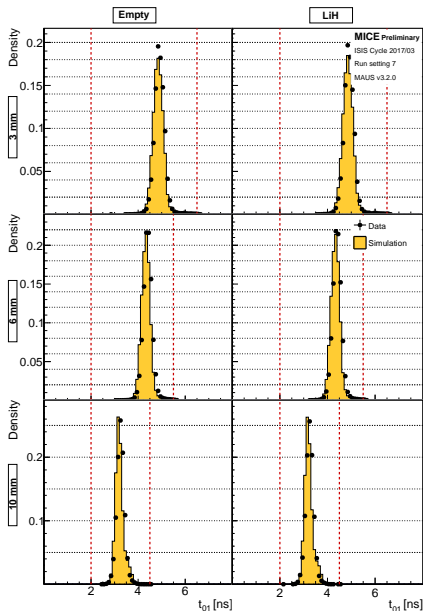
2017/02-7 data samples

Each number in the table below represents the amount of tracks that pass the row's cut and that cut alone. **All the data available is included**.

Cuts	No absorber			LiH absorber		
Input $\epsilon_\perp$	3 mm	6 mm	10 mm	3 mm	6 mm	10 mm
None	719334	1458158	1212980	677811	857507	1024734
TOF0 SP	613401	1216732	963969	569998	708432	802106
TOF1 SP	687660	1396488	1126896	646037	820382	946978
Time-of-flight	293958	563262	429728	272118	327895	355393
TKU track	271421	969672	623020	257795	576315	529450
TKU χ^2/ndf	252299	891481	574656	239333	527072	487189
TKU fiducial	268867	962979	595927	255364	572451	506443
TKU Momentum	81103	288399	132168	76067	168826	111180
Energy loss	119744	463164	266932	111700	269547	219638
All US	**54884**	**219146**	**87197**	**50602**	**126644**	**71213**
TKD track	53656	204415	60326	49056	118088	48193
TKD χ^2/ndf	52760	201679	59464	48361	116683	47676
TKD fiducial	53227	195329	51847	47928	114054	42774
All DS	**52368**	**192864**	**51203**	**47271**	**112777**	**42375**

Systematic uncertainties on the cooling measurement

Main sources of systematic uncertainty:

- tracker position offset (± 1 mm);
- tracker rotation offset (± 1 mrad);
- Deviation in CC current ($\pm 1\,\%$);
- Deviation in E1/E2 current ($\pm 5\,\%$);
- Unknown tracker glue density ($\pm 25\,\%$).

For each source, 10^6 muons resampled from the measured distribution. Same cuts applied to the so-produced simulation.
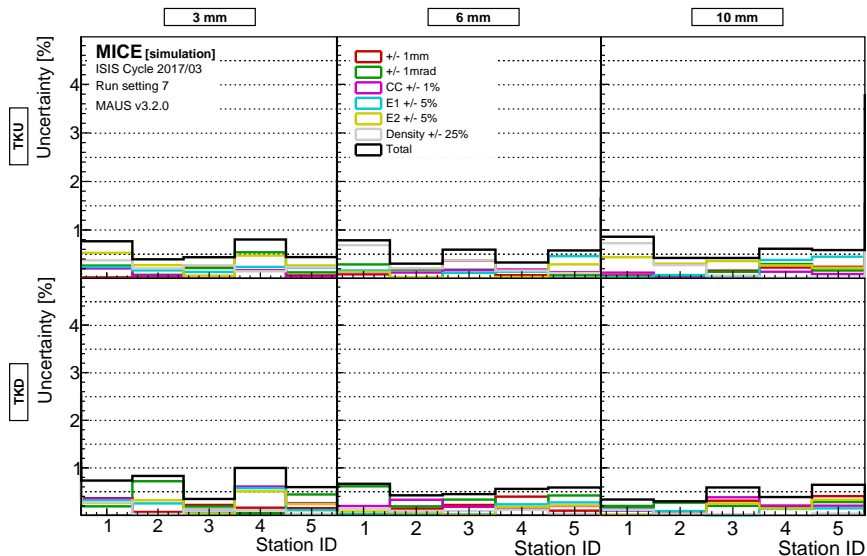
Each quantity represented is computed in each case and a systematic study of the uncertainty is produced.

Next slides show the effect on the amplitude distributions, the fractional emittance and the density estimation for 2017/02-7.

Amplitude distribution systematics
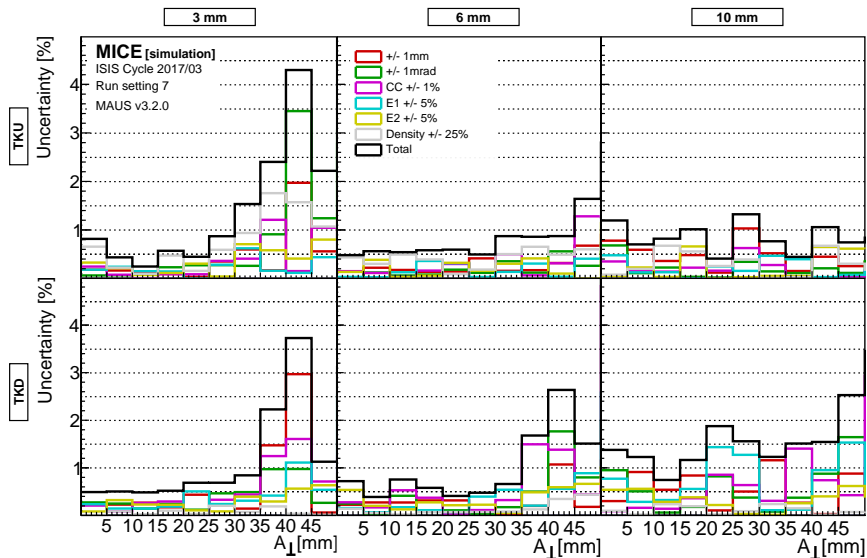
9 % fractional emittance systematics

Density levels systematics
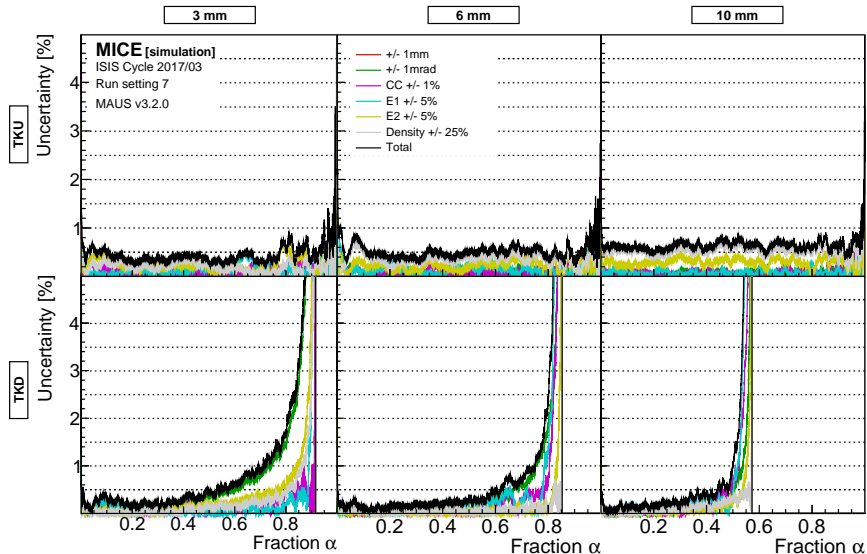
Density ratios in data
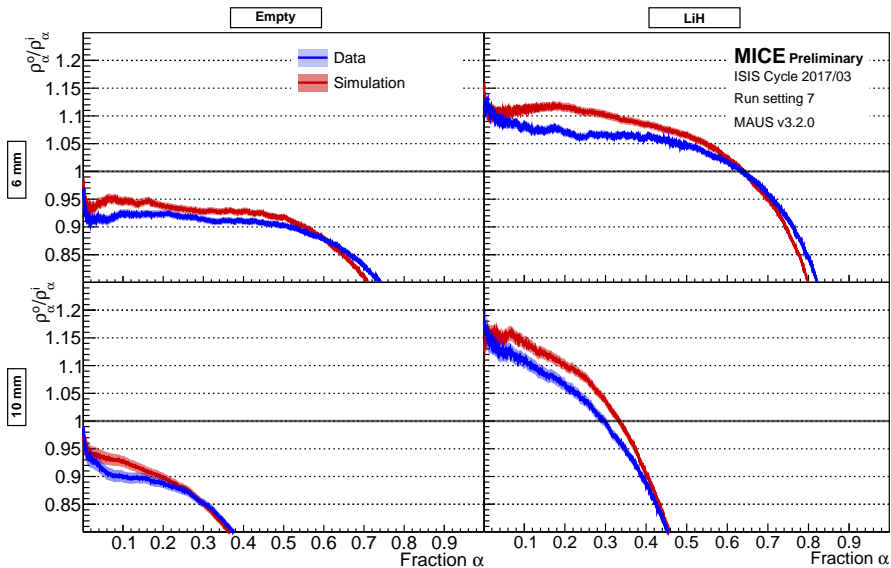
Electron-Muon Ranger

The Electron-Muon Ranger is a totally active tracker calorimeter made of 48 planes of 59 triangular bars in an alternating XY arrangement.

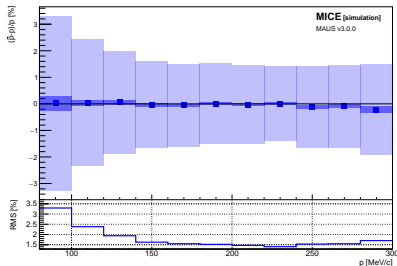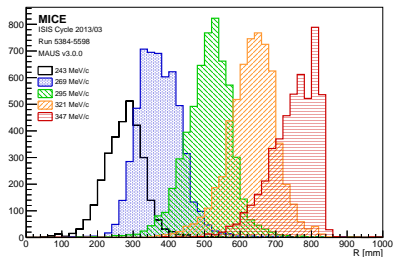Its function is to **tag muons that have decayed in flight inside the cooling channel**.
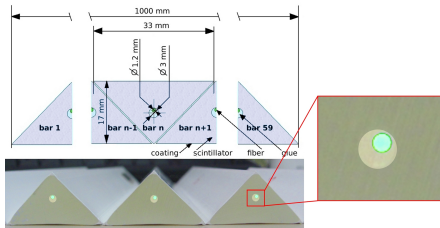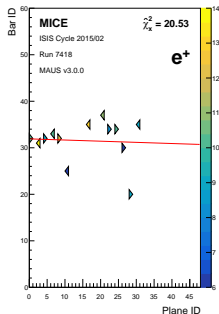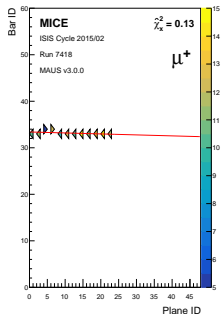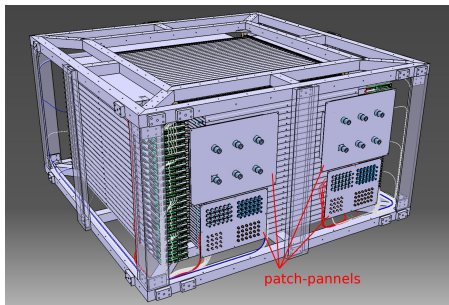
Electron-Muon Ranger muon momentum resolution

The muon range in the EMR is proportional to its momentum through

$$R = \int_{p_0}^{0} \frac{dp}{|dE/dx|} \beta c. \qquad (4)$$

The range is measured and the equation numerically inverted using the Bethe-Bloch formula to yield p_0.
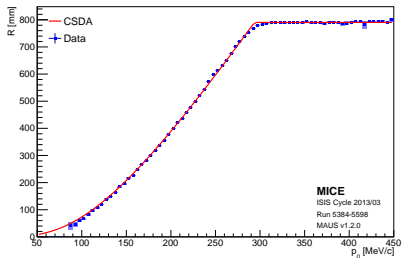
Electron-Muon Ranger $e^{\pm}$ rejection efficiency

Two $e^{\pm}$ identification variables

- Track continuity (density);
- Shower lateral spread (χ^2).

Used to build a multivariate selection of muons: **dense and compact**.

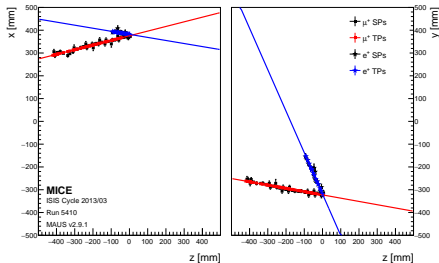Constrained contamination to $f_e < 0.09\%$ at 1σ C.L.
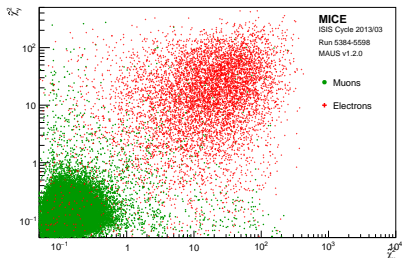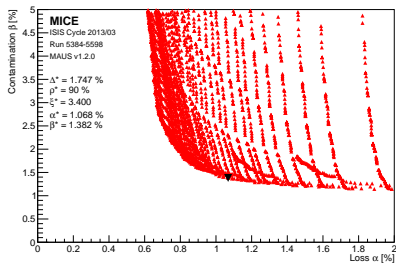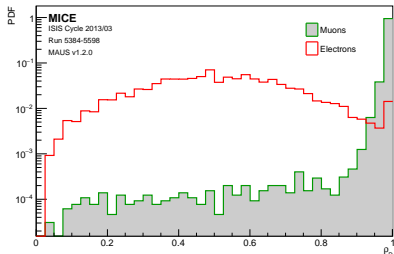
Electron-Muon Ranger decay matching

Reconstruct many decay parameters:

- Vertex position;
- Time between stop and decay;
- Relative orientation.

Feature used to demonstrate shorter negative muon lifetime and progressive beam depolarisation.
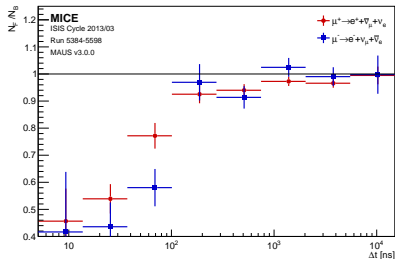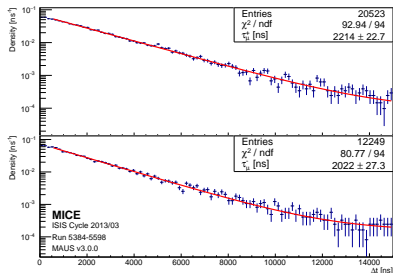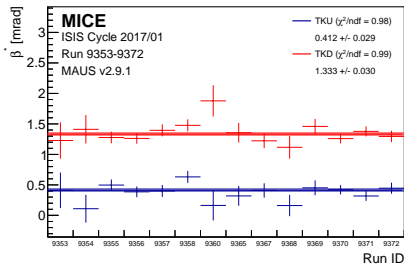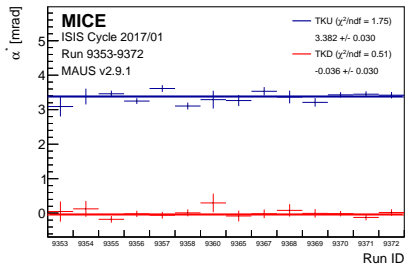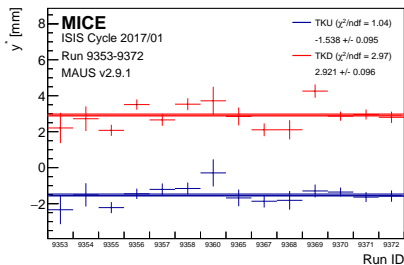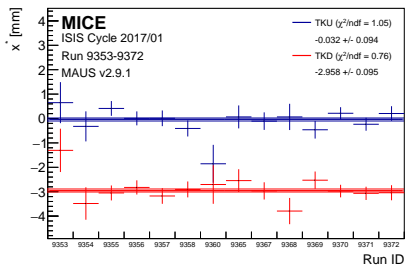
Beam-based detector alignment

The beam-based detector alignment algorithm was developed to reconstruct the position of the trackers, embedded in magnet bores.

The method uses the two time-of-flight detectors as a reference axis and reconstruct position through
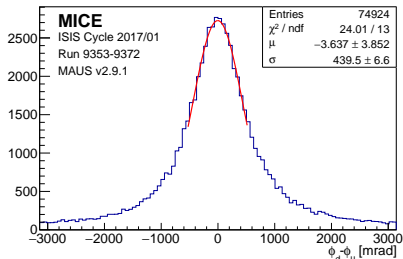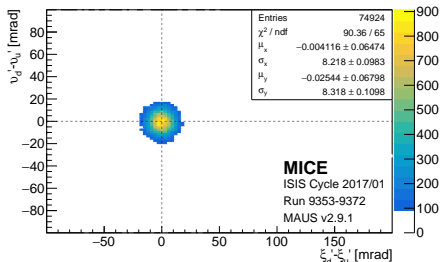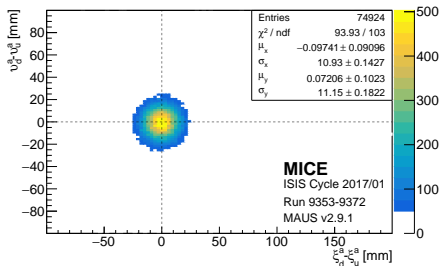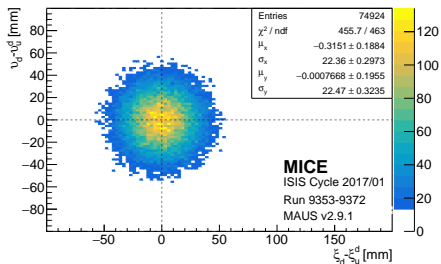
$$
\begin{cases}
x_T = -\langle x_t - \xi_{12}^t \rangle \\
y_T = -\langle y_t - \upsilon_{12}^t \rangle \\
\beta_T = -\langle x_t' - \xi_{12}' \rangle \\
\alpha_T = \langle y_t' - \upsilon_{12}' \rangle
\end{cases}
. \tag{5}
$$
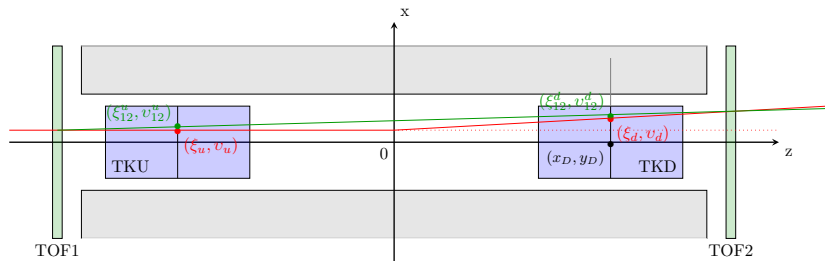
Alignment constants for the 2017/01 user cycle

Tracker alignment in the 2017/01 user cycle

PID detector alignment in the 2017/01 user cycle